Signal Processing 91 (2011) 1803–1811

Contents lists available at ScienceDirect

Signal Processing

journal homepage: www.elsevier.com/locate/sigpro

An ESPRIT-like algorithm for coherent DOA estimation based on data matrix decomposition in MIMO radar

Caicai Li, Guisheng Liao*, Shengqi Zhu, Sunyong Wu

National Laboratory of Radar Signal Processing, Xidian University, Xi'an, Shaanxi 710071, China

ARTICLE INFO

Article history:
Received 5 July 2010
Received in revised form
8 February 2011
Accepted 9 February 2011
Available online 19 February 2011

Keywords:
MIMO radar
Direction-of-arrival (DOA) estimation
ESPRIT
Coherent source

ABSTRACT

A direction-of-arrival (DOA) estimation method for coherent sources is presented for MIMO radar. It uses symmetrical array mode for both the transmit and receive arrays and reconstructs a special data matrix from the range-compressed receive data. In the reconstructed matrix, the signal term is a Toeplitz matrix with the rank only related to the DOAs of the signals and independent with their coherency. Taking the noise term into account, the average method of multiple pulses is utilized to obtain the signal and noise subspaces. And then the DOA can be resolved via the SVD-based ESPRIT algorithm. Furthermore, the presented method is also useful in spatial colored noise scenario for MIMO radar. Theoretical and numerical simulations show the effectiveness of the proposed algorithm.

1. Introduction

For the DOA estimation of narrowband signal sources, the subspace-based high resolution approaches such as MUSIC [1] and ESPRIT [2] have proven to be effective. However, when coherent or highly correlated signals exist, the rank loss of the covariance matrix results in the invalidity of these subspace-based methods. The conventional solution to this problem is spatial smoothing technique [3] and its improved approaches [4,5]. These methods eliminate the rank loss of the spatial covariance matrix, but they cannot equate it to the one of the independent sources and lead to large aperture loss, which degrades the estimation accuracy. The maximum likelihood (ML) method [6] which makes use of the probability distribution to estimate DOA can effectively avoid aperture loss, but it brings a serious computation load in practical application. Han and Zhang [7] proposed an ESPRIT-like algorithm, which finds the signal subspace and noise subspace by reconstructing a Toeplitz matrix from the covariance matrix of array output. Zeng and Liao [8] solved the coherent problem by data matrix decomposition, which is consistent with Ref. [7] in essence. In Refs. [7,8], the correlated sources are equated to the independent ones, in other words, the correlation of the sources are completely de-correlated, which will improve the performance to a certain extent. However, the aperture loss problem remains unresolved and the spatial colored noise circumstance is not considered.

In recent years, MIMO radar [9–18] has drawn considerable attention for its potential advantage over the conventional phased array radar. MIMO radar has multiple transmit antennas which emit orthogonal or partially correlated waveforms and multiple antennas receiving all the reflected signals. The receive data of each transmit waveform can be extracted from the mixed receive signal by a band of matched filters. MIMO radar is classified as two kinds by the configuration of the transmit and receive antennas: (1) the widely spaced MIMO radar [9,10] in which antennas of at least one of the transmit and receive arrays are widely spaced and (2) the closely spaced MIMO radar [11–18] (including mono-static and bi-static ones) in which antennas of both the transmit and receive arrays are closely spaced. The former aims at mitigating the

* Corresponding author. Tel.: +86 29 88201030.
E-mail address: gsliao@xidian.edu.cn (G. Liao).

0165-1684/$ - see front matter Crown Copyright © 2011 Published by Elsevier B.V. All rights reserved.
doi:10.1016/j.sigpro.2011.02.004

target scintillation effect by capitalizing on the spatial diversity. The latter seeks to maximize the degree of freedom (DoF) of radar system or realize transmit beamforming in the receive side. For independent sources, literatures [11–15] have studied parameter identifiability in mono-static MIMO radar and Refs. [16–18] have researched joint direction of departure (DOD) and DOA estimation in bi-static MIMO radar. In this paper, a DOA estimation method for correlated or coherent sources of mono-static MIMO radar is proposed, which can remedy the aperture loss while maintain the advantage of Refs. [7] and [8] by utilizing the large DoF of MIMO radar and is also useful in colored noise scenario by capitalizing on the character of the noise of MIMO radar.

In the presented method, symmetrical array mode is considered for both the transmit and receive arrays of mono-static MIMO radar and the data matrix decomposition method is employed to reconstruct a special matrix, of which the signal term is a Toeplitz matrix whose rank is only related to the DOA of the signals and is independent with their correlation. After being subtly processed using multiple pulses, the signal and noise terms can be separated successfully and the SVD-based ESPRIT algorithm is used to resolve the DOA. Owing to the property of the range-compressed noise of MIMO radar, the proposed method is useful in both the white and spatial colored noise environment. Since the correlation of the sources have no effect and the large DoF of MIMO radar is made good use of, the proposed method takes on good estimation accuracy in both the white and colored noise scenarios.

This paper is organized as follows. Section 2 reviews the mono-static MIMO radar signal model. In Section 3, the suggested algorithm is applied to, respectively, the transceiver system and independent transmitter and receiver system, with both the white noise and colored noise in consideration, and summarization of its steps is given at the last. Section 4 gives some theoretical analysis of the proposed method. And some numerical simulations are conducted to prove the effectiveness of the proposed method in Section 5. Finally, Section 6 concludes this paper.

2. Mono-static MIMO radar signal model

Consider a narrowband mono-static MIMO radar system of which both the transmit and receive arrays are uniform linear arrays (ULA) composed of $2M+1$ and $2N+1$ identical omnidirectional sensors, which are indexed as $-M,\ldots,0,\ldots M$ and $-N,\ldots,0,\ldots N$ separately, shown in Fig. 1 (in fact, the number of sensors does not have to be odd, herein we just take odd number for example). The corresponding inter-element spaces are d_t and d_r. Assume that all the transmit antennas simultaneously emit orthogonal coded continuous periodic waveforms, which have identical bandwidth and center frequency (see, e.g., Refs. [12–14,17–18]) and the wavelength is λ. The effect of Doppler frequencies on the orthogonality of waveforms and the variety of phases within repetition intervals can be ignored according to Ref. [19]. Let $\mathbf{s}_m \in \mathbf{C}^{1\times K}$ denotes the sampled baseband coded signal of the mth transmit antenna within one repetition interval and $\mathbf{s}_m\mathbf{s}_m^H = K$, where K is the length of the waveform sequence and $(\cdot)^H$ is the conjugate transposition. The target appears in the far-field and θ denotes the direction of the target with respect to the norm of the transmit and receive arrays. Under the simplifying assumption of point targets, the received data matrix of the lth pulse, denoted as $\mathbf{X}_l \in \mathbf{C}^{(2N+1)\times K}$ in Fig. 1, can be described by the equation

$$\mathbf{X}_l = \sum_{p=1}^{P} \mathbf{a}_r(\theta_p)\beta_p e^{j2\pi f_{d_p} t_l}\mathbf{a}_t(\theta_p)^T\mathbf{S} + \mathbf{W}_l \quad l = 1,2,\ldots L \tag{1}$$

where $(\cdot)^T$ denotes the transpose operator, p is the target index and P the number of targets. $\mathbf{a}_r(\theta)\in\mathbf{C}^{(2N+1)\times 1}$ and $\mathbf{a}_t(\theta)\in\mathbf{C}^{(2M+1)\times 1}$ are the steering vector of the receive and transmit arrays, respectively. $\beta \in C$ denotes the radar cross section (RCS) of the target and f_d Doppler frequency. t_l represents the slow time, l is the slow time index and L is the coherent pulse number. $\mathbf{W}\in\mathbf{C}^{(2N+1)\times K}$ denotes the noise matrix and columns of $\mathbf{W}$ are of independent and identically distributed (i.i.d) circularly symmetric complex Gaussian random vectors with zero mean and an unknown covariance matrix $\mathbf{Q}$ for each pulse. $\mathbf{A}_r = [\mathbf{a}_r(\theta_1),\mathbf{a}_r(\theta_2),\ldots,\mathbf{a}_r(\theta_P)]$ and $\mathbf{A}_t = [\mathbf{a}_t(\theta_1),\mathbf{a}_t(\theta_2),\ldots,\mathbf{a}_t(\theta_P)]$ are array manifold matrices. And

$$\mathbf{a}_r(\theta) = \left[e^{-j(2\pi/\lambda)Nd_r\sin\theta},\ldots,e^{-j(2\pi/\lambda)d_r\sin\theta},1,e^{j(2\pi/\lambda)d_r\sin\theta},\ldots,e^{j(2\pi/\lambda)Nd_r\sin\theta}\right]^T \tag{2}$$

$$\mathbf{a}_t(\theta) = \left[e^{-j(2\pi/\lambda)Md_t\sin\theta},\cdots,e^{-j(2\pi/\lambda)d_t\sin\theta},1,e^{j(2\pi/\lambda)d_t\sin\theta},\cdots,e^{j(2\pi/\lambda)Md_t\sin\theta}\right]^T \tag{3}$$

$$\mathbf{S} = \left[\mathbf{s}_{-M}^T,\ldots,\mathbf{s}_{-1}^T,\mathbf{s}_0^T,\mathbf{s}_1^T,\ldots,\mathbf{s}_M^T\right]^T \tag{4}$$

According to the orthogonal property of the transmit waveforms, we obtain

$$\mathbf{R}_{ss} = \frac{1}{K}\mathbf{S}\mathbf{S}^H = \mathbf{I}_{(2M+1)\times(2M+1)} \tag{5}$$

After range-compression using $\mathbf{S}^H(\mathbf{S}\mathbf{S}^H)^{-1/2}$, range-compressed data matrix $\mathbf{Y}_l\in\mathbf{C}^{(2N+1)\times(2M+1)}$ in Fig. 1 can be written as

$$\begin{aligned}\mathbf{Y}_l &= \mathbf{A}_r\Lambda_l\mathbf{A}_t{}^T + \mathbf{N}_l \\ &= [\mathbf{y}_{-Ml},\ldots,\mathbf{y}_{0l},\ldots,\mathbf{y}_{Ml}] \quad l = 1,2,\ldots L\end{aligned} \tag{6}$$

where $\mathbf{y}_{il}^{(2N+1)\times 1}$represent the receive data that range-compressed by the ith transmit antenna. And

$$\Lambda_l = diag(\mathbf{b}_l), \quad \mathbf{b}_l = \sqrt{K}[\beta_1 e^{j2\pi f_{d_1} t_l},\beta_2 e^{j2\pi f_{d_2} t_l},\ldots,\beta_P e^{j2\pi f_{d_p} t_l}]^T \tag{7}$$

$$\begin{aligned}\mathbf{N}_l &= \mathbf{W}_l\mathbf{S}^H(\mathbf{S}\mathbf{S}^H)^{-1/2} \\ &= \frac{1}{\sqrt{K}}\left[\mathbf{W}_l\mathbf{s}_{-M}^H,\ldots,\mathbf{W}_l\mathbf{s}_1^H,\mathbf{W}_l\mathbf{s}_0^H,\mathbf{W}_l\mathbf{s}_1^H,\ldots,\mathbf{W}_l\mathbf{s}_M^H\right] \\ &= [\mathbf{n}_{-Ml},\ldots,\mathbf{n}_{-1l},\mathbf{n}_{0l},\mathbf{n}_{1l},\ldots,\mathbf{n}_{Ml}]\end{aligned} \tag{8}$$

where $diag(\cdot)$ denotes a diagonal matrix whose main diagonal is equal to a vector or a vector consisting of the main diagonal of a matrix.

The cross-covariance matrices of $\mathbf{n}_{il}$ and $\mathbf{n}_{jl}$ are formulated as follows:

$$\begin{aligned} E(\mathbf{n}_{il}\mathbf{n}_{jl}^H) &= E\left[\left(\frac{1}{\sqrt{K}}\mathbf{W}_l\mathbf{s}_i^H\right)\left(\frac{1}{\sqrt{K}}\mathbf{W}_l\mathbf{s}_j^H\right)^H\right] \\ &= \frac{1}{K}E\left\{[\mathbf{s}_i^*\otimes\mathbf{I}_N]vec(\mathbf{W}_l)vec^H(\mathbf{W}_l)[\mathbf{s}_j^T\otimes\mathbf{I}_N]\right\} \\ &= \frac{1}{K}[\mathbf{s}_i^*\otimes\mathbf{I}_N]E[vec(\mathbf{W}_l)vec^H(\mathbf{W}_l)]\left[\mathbf{s}_j^T\otimes\mathbf{I}_N\right] \\ &= \frac{1}{K}(\mathbf{s}_i^*\otimes\mathbf{I}_N)(\mathbf{I}_K\otimes\mathbf{Q})(\mathbf{s}_j^T\otimes\mathbf{I}_N) \\ &= \frac{1}{K}\mathbf{s}_i^*\mathbf{s}_j^T\otimes\mathbf{Q} = \begin{cases}\mathbf{Q}, & i=j \\ \mathbf{0}, & i\neq j\end{cases} \quad i,j=-M,\ldots,0,\ldots,M \end{aligned} \tag{9}$$

where $E(\cdot)$, $(\cdot)^*$, $\otimes$ and $vec(\cdot)$ denote the expectation, the complex conjugate, the Kronecker product and the vectorization operator, respectively.

In what have discussed above, the general signal model of mono-static MIMO radar is given. The targets in it can be independent or correlated, which depends on the cross-correlation of their *RCSs*. Taking two targets for example, if their cross-correlation coefficient equals zero, they are independent; and otherwise they are correlated. In particular, if the cross-correlation coefficient equals unity, they are coherent. Correlated or coherent signals are often encountered in multipath or some other scenarios. DOA estimation of correlated or coherent sources is a topic attracting much attention of researchers. A number of coherent DOA estimation methods [3–8] in phased array radar have been proposed, as discussed in the former.

In this paper, we emphasize on the study of the DOA estimation in multipath scenario for in MIMO radar. Since multipath signals arise from the different propagation paths of the same target, their Doppler frequencies are identical and their *RCSs* are correlated random variables. For expression simplicity, we discuss the coherent signals with different complex amplitudes in what follows. Thus $\mathbf{b}_l$ in Eq. (7) can be rewritten as $\mathbf{b}_l=\sqrt{K}e^{j2\pi f_d t_l}[\alpha_1\beta,\alpha_2\beta,\alpha_3\beta,\ldots,\alpha_P\beta]^T$ where α_p represents the complex amplitude of the pth *RCS*. Assume β is a random variable submits to Rayleigh distribution with second order moment $E(\beta\beta^*)=\delta^2$ and obeys Swerling 2 mode. The first *RCS* is generally designated as the reference and thus $\alpha_1=1$.

In the following section, the proposed new algorithm will be described in detail. It is worth noting that compared with many classical DOA estimation methods, e.g. MUSIC, Capon, APES and GLRT [15], which need a single pulse only, the presented method requires a number of pulses, because in MIMO radar the received data are often range-compressed firstly for the purpose of enlarging the DoF of radar system.

3. New algorithm for DOA estimation of coherent sources

In mono-static MIMO radar system, two typical configurations (see, e.g., Refs. [12,14]) are often discussed: (1) the transceiver radar system in which the transmit and receive antennas occupy the same phase center with inter-element space of $\lambda/2$. This configuration is almost the same with the critically sampled phased array radar except that the transmit antennas emit different waveforms other than the scaled waveforms. It has the advantages of easily understanding, simplicity and low cost in hardware devices, but its virtual aperture is not adequately large because many of the virtual antenna locations are overlapped; (2) the independent transmitter and receiver radar system with the transmit and receive inter-element spaces of $(2N+1)\lambda/2$ and $\lambda/2$, respectively, where $2N+1$ is the number of the receive antennas. It turns out that this configuration possesses the largest contiguous virtual aperture of MIMO radar, which can observably improve the DOA estimation accuracy and increase the number of detected targets. However, since the transmit and receive antennas are independent, this configuration is complicated in implementation and high cost in practical application. Considering the colored noise case, a transmit antenna which is indexed by $-M-1$ in Fig. 1 is added for noise eliminating according to the noise property in Eq. (9). The new algorithm for the two typical configurations is presented as follows, with both the white and colored noise in consideration.

3.1. New algorithm for the transceiver MIMO radar

When the transceiver system is adopted, the locations of many virtual elements are superposed. Generally the excrescent virtual elements should be wiped off and only the effective virtual aperture is useful. In the proposed method, all the range-compressed data can be used, which reduces the computation load. Since the transmit and receive antennas are located at the same place, the array manifold matrix satisfies $\mathbf{A}_t^{(2M+1)\times P}=\mathbf{A}_r^{(2M+1)\times P}$, mark $\mathbf{A}_t$ and $\mathbf{A}_r$ by $\mathbf{A}^{(2M+1)\times P}$ for express clarity, Eq. (6) can be rewritten as

$$\mathbf{Z}_l=\mathbf{Y}_l=\mathbf{A}\mathbf{\Lambda}_l\mathbf{A}^T+\mathbf{N}_l \quad l=1,2,\ldots L \tag{10}$$

Assume that $\mathbf{J}^{(2M+1)\times(2M+1)}$ is an exchange matrix of which the elements on the main anti-diagonal are ones and the others are zeros, we can obtain

$$\begin{aligned} \mathbf{Z}_{1l} &= \mathbf{J}\mathbf{Z}_l=\mathbf{J}\mathbf{A}\mathbf{\Lambda}_l\mathbf{A}^T+\mathbf{J}\mathbf{N}_l \\ &= \mathbf{B}\mathbf{\Lambda}_l\mathbf{B}^H+\mathbf{N}_{1l} \end{aligned} \tag{11}$$

where

$$\mathbf{B}=\mathbf{J}\mathbf{A}=[\mathbf{b}(\theta_1),\mathbf{b}(\theta_2),\ldots,\mathbf{b}(\theta_P)] \tag{12}$$

$$\mathbf{b}(\theta_i)=\mathbf{J}\mathbf{a}(\theta_i)=\left[e^{j\pi M\sin\theta_i},\ldots,e^{j\pi\sin\theta_i},1,e^{-j\pi\sin\theta_i},\ldots,e^{-j\pi M\sin\theta_i}\right]^T \tag{13}$$

Without considering the noise, it can be seen that Eq. (11) is a Hermitian Toeplitz matrix the rank of which only relates to the DOAs of the signals and is independent with their correlation. In other words, Eq. (11) achieves complete de-correlation. Considering the noise, the following average method can be used, and the details for the Gaussian white and the Gaussian spatial colored noise circumstances are presented in the following Section A and B, respectively.

Section A, Gaussian white noise case. In the presence of Gaussian white noise with zero mean and variance δ_n^2, δ_n^2 can be estimated by the small eigenvalues of the covariance matrix. Based on this, the noise term can be subtracted as follows:

$$\begin{aligned}\overline{\mathbf{Z}}_1 &= E\{\mathbf{Z}_{1l}^*(1,1)\mathbf{Z}_{1l}\}\\ &= \mathbf{B}E\left[(\sqrt{K}e^{-j2\pi f_d t_l}\beta^*\sum_{p=1}^{P}\alpha_p^*)\mathbf{\Lambda}_l\right]\mathbf{B}^H + E[\mathbf{N}_{1l}^*(1,1)\mathbf{N}_{1l}]\\ &= \mathbf{B}\overline{\mathbf{\Lambda}}\mathbf{B}^H + \overline{\mathbf{N}} \approx \frac{1}{L}\sum_{l=1}^{L}\mathbf{Z}_{1l}^*(1,1)\mathbf{Z}_{1l}\end{aligned} \tag{14}$$

where $\mathbf{Z}(i,j)$ represents the (i,j)th element of matrix $\mathbf{Z}$. It is necessary to point out that any element of $\mathbf{Z}_{1l}$ can be chosen to obtain $\overline{\mathbf{Z}}_1$, and the only difference is that the expression of $\overline{\mathbf{\Lambda}}$ and $\overline{\mathbf{N}}$ should be slightly changed

$$\overline{\mathbf{\Lambda}} = diag(\overline{\mathbf{b}}) \tag{15}$$

$$\overline{\mathbf{b}} = [\overline{b}_1, \overline{b}_2, \ldots, \overline{b}_P]^T \tag{16}$$

$$\begin{aligned}\overline{b}_i &= KE(\beta\beta^*)\sum_{p=1}^{P}\alpha_p^*\alpha_i = K\delta^2\sum_{p=1}^{P}\alpha_p^*\alpha_i\\ &= K\delta^2|\alpha_i|^2 + K\delta^2\sum_{p=1,p\neq i}^{P}\alpha_p^*\alpha_i\end{aligned} \tag{17}$$

$$\overline{\mathbf{N}} = \begin{bmatrix}\delta_n^2 & \mathbf{0}\\ \mathbf{0} & \mathbf{0}\end{bmatrix}_{(2M+1)\times(2M+1)} \tag{18}$$

The expression of $\overline{\mathbf{N}}$ in Eq. (18) derives from the noise property of MIMO radar in Eq. (9). By averaging the small eigenvalues of $\hat{\mathbf{R}} = (1/L)\sum_{l=1}^{L} vec(\mathbf{Y}_l)vec(\mathbf{Y}_l)^H$, the noise power δ_n^2 can be estimated and thus $\overline{\mathbf{N}}$ can be determined. Then the noise free equivalent covariance matrix $\mathbf{C}$ can be obtained as follows:

$$\mathbf{C} = \overline{\mathbf{Z}}_1 - \overline{\mathbf{N}} = \mathbf{B}\overline{\mathbf{\Lambda}}\mathbf{B}^H \tag{19}$$

From Eq. (17), it can be seen that the value of $\overline{b}_i$ depends on the complex amplitudes of the *RCSs* and does not equal zero in general. Under the assumption that $\overline{b}_i \neq 0, i = 1,2,P$, we can conclude that matrix $\mathbf{C}$ is equivalent to the noise free spatial covariance matrix of P independent sources. Consequently classical subspace-based methods can be applied to $\mathbf{C}$ directly.

For the usage of numerical ESPRIT method, we construct two matrices $\mathbf{C}_1$ and $\mathbf{C}_2$ by the first $2M$ and the last $2M$ columns of $\mathbf{C}$, respectively, denoted as

$$\mathbf{C}_1 = \mathbf{B}\overline{\mathbf{\Lambda}}\mathbf{B}_1^H, \quad \mathbf{C}_2 = \mathbf{B}\overline{\mathbf{\Lambda}}\mathbf{\Phi}\mathbf{B}_1^H \tag{20}$$

where $\mathbf{B}_1$ consists of the first $2M$ rows of $\mathbf{B}$, and

$$\mathbf{\Phi} = diag(\boldsymbol{\varphi}), \quad \boldsymbol{\varphi} = [e^{j\pi\sin\theta_1}, e^{j\pi\sin\theta_2}, \ldots, e^{j\pi\sin\theta_P}]^T \tag{21}$$

As has discussed above, the value of $\overline{b}_i$ does not equal zero in general. Under the condition that $\overline{b}_i \neq 0, i = 1,2\ldots P$, $rank(\overline{\mathbf{\Lambda}}) = P$, where $rank(\cdot)$ denotes the rank of a matrix. Meanwhile, since $\mathbf{B}_1$ and $\mathbf{B}$ are Vandermonde matrices with rank P and $\mathbf{\Phi}$ is a diagonal matrix also with the rank P, we can conclude that $rank(\mathbf{C_1}) = rank(\mathbf{C_2}) = P$. Assume that γ is a complex constant, then

$$\mathbf{C_1} - \gamma\mathbf{C_2} = \mathbf{B}\mathrm{Re}(\overline{\mathbf{\Lambda}})(\mathbf{I} - \gamma\mathbf{\Phi})\mathbf{B}_1^T \text{ and } rank(\mathbf{C_1} - \gamma\mathbf{C_2}) = rank(\mathbf{I} - \gamma\mathbf{\Phi}) \tag{22}$$

From Eq. (22), it can be concluded that if and only if $\gamma = e^{-j\pi\sin\theta_p}, p = 1,2,\ldots P$, the matrix $\boldsymbol{I} - \gamma\mathbf{\Phi}$ is singular. Consequently searching for γ, we can get $e^{-j\pi\sin\theta_p}$, $p = 1,2,\ldots P$. Herein the SVD-based ESPRIT method [20] can be adopted to estimate the direction of the P coherent targets. The details are as follows: first, compute the SVD of $\mathbf{C}_1$

$$\mathbf{C_1} = \mathbf{U}\sum\mathbf{V}^H = [\mathbf{U}_1, \mathbf{U}_2]\begin{bmatrix}\sum_1 & \mathbf{0}\\ \mathbf{0} & \sum_2\end{bmatrix}\begin{bmatrix}\mathbf{V}_1^H\\ \mathbf{V}_2^H\end{bmatrix} \tag{23}$$

where $\sum_1$ consists of P principal singular values.

And then compute the P values of general eigenvalues (GE's), say, $\eta_p's$, of the matrix pencil $\left\{\sum_1, \mathbf{U}_1^H\mathbf{C}_2\mathbf{V}_1^H\right\}$. The DOAs are given by

$$\theta_p = 180\cdot\mathrm{asin}(ang(\eta_p^*)/\pi)/\pi, p = 1,2,\ldots P \tag{24}$$

where $ang(\cdot)$ is the operation which returns the phase angles, in radians, for each element of a complex matrix. The angles lie between $\pm\pi$. And $asin(\cdot)$ represents the inverse sine (arcsine) operation.

Section B, Gaussian spatial colored noise case. In Gaussian spatial colored noise environment, since the noise covariance matrix $\mathbf{Q}$ cannot be estimated, the noise term cannot be subtracted like Eq. (19). But it is known from Eq. (9) that the noise range-compressed by different orthogonal waveforms is independent, which enables us to eliminate the colored noise by adding a transmit antenna, as shown in Fig. 1. The range-compressed receive data of the added transmit antenna can be expressed by

$$\mathbf{y}_{-M-1l} = \mathbf{A}_r\mathbf{\Lambda}_l diag(\mathbf{\Phi}^{-M-1}) + \mathbf{n}_{-M-1l} \tag{25}$$

According to Eq. (9), we can choose any element or the mean value of $\mathbf{y}_{-M-1l}$ to deal with the noise term in Eq. (14). Without generality, herein we choose the first element of $\mathbf{y}_{-M-1l}$, denoted by $\mathbf{y}_{-M-1l}(1,1) = \sqrt{K}e^{j2\pi f_d t_l}\beta\sum_{p=1}^{P}\alpha_p e^{-j\pi(2M+1)\sin\theta_p} + n_{-M-1l}(1,1)$ to process the noise term, thus

$$\begin{aligned}\overline{\mathbf{Z}}_1 &= E\{\mathbf{y}_{-M-1l}^*(1,1)\mathbf{Z}_{1l}\}\\ &= \mathbf{B}E\left[\left(\sqrt{K}e^{-j2\pi f_d t_l}\beta^*\sum_{p=1}^{P}\alpha_p^* e^{j\pi(2M+1)\sin\theta_p}\right)\mathbf{\Lambda}_l\right]\mathbf{B}^H + E[\mathbf{n}_{-M-1l}^*(1,1)\mathbf{N}_{1l}]\\ &= \mathbf{B}\overline{\mathbf{\Lambda}}_1\mathbf{B}^H \approx \frac{1}{L}\sum_{l=1}^{L}\mathbf{y}_{-M-1l}^*(1,1)\mathbf{Z}_{1l}\end{aligned} \tag{26}$$

where

$$\overline{\mathbf{\Lambda}}_1 = diag(\overline{\mathbf{b}}_1) \tag{27}$$

$$\overline{\mathbf{b}}_1 = [\overline{b}_{1_1}, \overline{b}_{1_2}, \ldots, \overline{b}_{1_P}]^T \tag{28}$$

$$\begin{aligned}\overline{b}_{1_i} &= KE(\beta\beta^*)\sum_{p=1}^{P}\alpha_p^*\alpha_i e^{-j\pi(2M+1)\sin\theta_p}\\ &= K\delta^2\sum_{p=1}^{P}\alpha_p^*\alpha_i e^{-j\pi(2M+1)\sin\theta_p}\\ &= K\delta^2|\alpha_i|^2 + K\delta^2\sum_{p=1,p\neq i}^{P}\alpha_p^*\alpha_i e^{-j\pi(2M+1)\sin\theta_p}\end{aligned} \tag{29}$$

From Eq. (26), it can be seen that the colored noise term is successfully eliminated, and we get

$$\mathbf{C}=\overline{\mathbf{Z}}_1=\mathbf{B}\overline{\mathbf{\Lambda}}_1\mathbf{B}^H \tag{30}$$

And then the DOA can be resolved using Eqs. (20)–(24).

3.2. New algorithm for the independent transmitter and receiver MIMO radar

When the independent transmitter and receiver system is adopted, $\mathbf{A}_t\neq\mathbf{A}_r$. $\mathbf{Y}_l$ in Eq. (6) cannot be used directly to realize complete de-correlation, because the transmit array does not satisfy the Nyquist sampling theorem, which will lead to phase ambiguity and inaccurate DOA estimation. To avoid the phase ambiguity and make good use of MIMO radar's large DoF, we firstly stack the columns of $\boldsymbol{Y}_l$ in Eq. (6) into a vector $\mathbf{y}_l$, and then form the constructed matrix from $\boldsymbol{y}_l$ using the method in Ref. [8].

First, by stacking the columns of $\boldsymbol{Y}_l$ in Eq. (6) into a vector, we have

$$\mathbf{y}_l=vec(\mathbf{Y}_l)=[\mathbf{y}_{-Ml}^T,\ldots,\mathbf{y}_{0l}^T,\ldots,\mathbf{y}_{Ml}^T]^T=\mathbf{A}_{rt}\mathbf{b}_l+\mathbf{n}_l\quad l=1,2,\ldots L \tag{31}$$

where

$$\mathbf{A}_{rt}=[\mathbf{a}_{rt}(\theta_1),\mathbf{a}_{rt}(\theta_2),\ldots,\mathbf{a}_{rt}(\theta_P)] \tag{32}$$

$$\mathbf{a}_{rt}(\theta_i)=\mathbf{a}_t(\theta_i)\otimes\mathbf{a}_r(\theta_i)=[e^{-jI\pi\sin\theta_i},\ldots,1,\ldots,e^{jI\pi\sin\theta_i}]^T \tag{33}$$

where $I=2MN+M+N$, and

$$\mathbf{n}=[\mathbf{n}_{-Ml}^T,\ldots,\mathbf{n}_{0l}^T,\ldots,\mathbf{n}_{Ml}^T]^T \tag{34}$$

Then by the method in Ref. [8], $\boldsymbol{Z}_l$ is constructed as follows:

$$\begin{aligned}\mathbf{Z}_l&=[\mathbf{y}_l(1:F),\mathbf{y}_l(2:F+1),\ldots,\mathbf{y}_l(V-F+1:V)]\\&=\mathbf{A}_1[\mathbf{b}_l,\mathbf{\Phi}\mathbf{b}_l,\mathbf{\Phi}^2\mathbf{b}_l,\ldots,\mathbf{\Phi}^{V-F}\mathbf{b}_l]+\mathbf{N}_l^z=\mathbf{A}_1\mathbf{\Lambda}_l\mathbf{A}_1^T+\mathbf{N}_l^z\quad l=1,2,\ldots L\end{aligned} \tag{35}$$

where $\mathbf{y}_l(m{:}n)$ is a section of $\boldsymbol{y}_l$ starting from the mth element and ending at the nth one. $V=(2M+1)(2N+1)$ is the length of the useful virtual aperture. F is a positive integer which satisfies the condition that $F>P$ and $V-F+1>P$. Herein we set $F=\lceil V/2\rceil$, where $\lceil\rceil$ denotes the smallest integer greater than or equal to a given number, for the purpose of obtaining the maximum detectable number. $\mathbf{A}_1$ consists of the first F (herein $F=\lceil V/2\rceil=V-F+1=I+1$) rows of the array manifold matrix $\mathbf{A}_{rt}$, and $\mathbf{N}_l^z=[\mathbf{n}_l(1:F),\mathbf{n}_l(2:F+1),\ldots,\mathbf{n}_l(V-F+1:V)]$.

Assume $\mathbf{J}^{F\times F}$ is the exchange matrix, we can obtain

$$\mathbf{Z}_{1l}=\mathbf{J}\mathbf{Z}_l=\mathbf{J}\mathbf{A}_1\mathbf{\Lambda}_l\mathbf{A}_1{}^T+\mathbf{J}\mathbf{N}_l^z=\mathbf{B}_2\mathbf{\Lambda}_l\mathbf{B}_2^H+\mathbf{N}_{1l}^z \tag{36}$$

where

$$\mathbf{B}_2=\mathbf{J}\mathbf{A}_1 \tag{37}$$

In white noise case, upon processing $\mathbf{Z}_{1l}$ by means of Eq. (14), we have

$$\begin{aligned}\overline{\mathbf{Z}}_1&=E\{\mathbf{Z}_{1l}^*(1,1)\mathbf{Z}_{1l}\}\\&=\mathbf{B}_2E\left[\left(\sqrt{K}e^{-j2\pi f_d t_l}\beta^*\sum_{p=1}^{P}\alpha_p^*\right)\mathbf{\Lambda}_l\right]\mathbf{B}_2^H+E(\mathbf{N}_{1l}^{z*}(1,1)\mathbf{N}_{1l}^z)\\&=\mathbf{B}_2\overline{\mathbf{\Lambda}}\mathbf{B}_2^H+\overline{\mathbf{N}}_1\approx\frac{1}{L}\sum_{l=1}^{L}\mathbf{Z}_{1l}^{z*}(1,1)\mathbf{Z}_{1l}^z\end{aligned} \tag{38}$$

where

$$\overline{\mathbf{N}}_1=\delta_n^2\mathbf{I}^{F\times F} \tag{39}$$

$\boldsymbol{I}$ is an identity matrix. And then the DOA can be obtained like Eqs. (19)–(24).

In colored noise case, the colored noise term can be treated like Eqs. (25)–(30), and the DOA can be obtained like Eqs. (20)–(24).

3.3. Steps of the proposed method

Step1: Obtain the range-compressed receive data $\mathbf{Y}_l$ in Eq. (6).
Step2: Construct the matrix $\mathbf{Z}_l$ from $\mathbf{Y}_l$ according to Eq. (10) or (35).
Step3: Evaluate matrix $\overline{\mathbf{Z}}_1$ using multiple pulses by Eq. (14) or (26) or (38).
Step4: In white noise environment, estimate the noise power δ_n^2 by averaging the small eigenvalues of the covariance matrix $\hat{\mathbf{R}}=(1/L)\sum_{l=1}^{L}vec(\mathbf{Y}_l)vec(\mathbf{Y}_l)^H$, and obtain the noise-free matrix $\mathbf{C}$ by Eq. (19). For colored noise, obtain $\mathbf{C}$ by Eq. (30).
Step5: Obtain $\mathbf{C}_1$ and $\mathbf{C}_2$ according to Eq. (20) and use the SVD-based ESPRIT method to estimate DOA of the coherent sources.

4. Theoretical analysis of the proposed method

In this subsection, some theoretical analysis of the proposed method is given. Firstly, we prove that the correlation of the sources has no effect on the rank of the noise free reconstructed matrix $\mathbf{C}_1$ and $\mathbf{C}_2$, and on the signal and noise subspaces obtained from them. And then the maximum detectable number is analyzed.

4.1. Analysis of the signal and noise subspaces

Without generality, we take $\mathbf{C}_1$ in formula (20) for example. Since $\mathbf{B}$ and $\mathbf{B}_1$ are Vandermonde matrices and $2M+1>P$, $2M>P$, then $rank(\mathbf{B})=rank(\mathbf{B}_1)=P$. Under the condition that $\bar{b}_i\neq0, i=1,2\ldots P$, it can be known that $rank(\overline{\mathbf{\Lambda}})=P$. Then it can be obtained that $rank(\mathbf{C}_1)=P$. So the rank of the noise free reconstructed matrix $\mathbf{C}_1$ is P, which has no relation with the correlation of the sources. Then $\mathbf{C}_1$ can be rewritten as

$$\begin{aligned}\mathbf{C}_1&=[\mathbf{u}_1,\ldots,\mathbf{u}_{2M+1}]\begin{bmatrix}\mathbf{\Sigma}&\mathbf{0}\\\mathbf{0}&\mathbf{0}\end{bmatrix}[\mathbf{v}_1,\ldots,\mathbf{v}_{2M}]^H\\&=[\mathbf{u}_1,\ldots,\mathbf{u}_P]\mathbf{\Sigma}[\mathbf{v}_1,\ldots,\mathbf{v}_P]^H\end{aligned} \tag{40}$$

where $\{\mathbf{u}_i,\ i=1,\ldots,2M+1\}$ and $\{\mathbf{v}_j,\ j=1,\ldots,2M\}$ are orthogonal vector sets consisting of the left and right singular vectors of $\mathbf{C}_1$, respectively. $\mathbf{\Sigma}=diag(\sigma_1,\sigma_2,\ldots,\sigma_P)$ and $\sigma_p,\ p=1,2,\ldots,P$ are singular values of $\mathbf{C}_1$. For any $\mathbf{u}_i\in span\{\mathbf{u}_{P+1},\ldots,\mathbf{u}_{2M+1}\}$ where $span\{\cdot\}$ denotes a space consisting of given vectors, we have

$$\mathbf{u}_i^H\mathbf{C}_1=\mathbf{u}_i^H[\mathbf{u}_1,\ldots,\mathbf{u}_P]\mathbf{\Sigma}[\mathbf{v}_1,\ldots,\mathbf{v}_P]^H=\mathbf{0} \tag{41}$$

$\mathbf{u}_i^H\mathbf{C}_1$ can also be written as

$$\mathbf{u}_i^H\mathbf{C}_1=\mathbf{u}_i^H\mathbf{B}\overline{\mathbf{\Lambda}}\mathbf{B}_1^H=\mathbf{u}_i^H[\mathbf{b}(\theta_1),\ldots,\mathbf{b}(\theta_P)]\overline{\mathbf{\Lambda}}[\mathbf{b}_1(\theta_1),\ldots,\mathbf{b}_1(\theta_P)]^H$$
$$=\sum_{p=1}^{P}[\mathbf{u}_i^H\mathbf{b}(\theta_p)\overline{b}_p]\mathbf{b}_1(\theta_p)=\mathbf{0} \quad (42)$$

where $\mathbf{b}_1(\theta_p)$ denotes the pth column of $\mathbf{B}_1$. Since $\{\mathbf{b}_1(\theta_1),\ldots,\mathbf{b}_1(\theta_P)\}$ are linear independent vectors, we have $\mathbf{u}_i^H\mathbf{b}(\theta_p)\overline{b}_p=\mathbf{0}$. Under the assumption that $\overline{b}_p\neq 0$, it can be obtained

$$\mathbf{u}_i^H\mathbf{b}(\theta_p)=0 \quad (43)$$

Thus we get

$$span\{\mathbf{u}_{P+1},\cdots,\mathbf{u}_{2M+1}\}\perp span\{\mathbf{b}(\theta_1),\ldots,\mathbf{b}(\theta_P)\} \quad (44)$$

From Eq. (44) it can be known that $\{\mathbf{b}(\theta_1),\ldots,\mathbf{b}(\theta_P),\mathbf{u}_{P+1},\cdots,\mathbf{u}_{2M+1}\}$ is a set of basis of $2M+1$ dimensional space. Since $\{\mathbf{u}_1,\ldots,\mathbf{u}_P,\mathbf{u}_{P+1},\ldots,\mathbf{u}_{2M+1}\}$ is a set of orthogonal basis of $2M+1$ dimensional space, it can be concluded that

$$span\{\mathbf{b}(\theta_1),\ldots,\mathbf{b}(\theta_P)\}=span\{\mathbf{u}_1,\ldots,\mathbf{u}_P\}$$
$$\perp span\{\mathbf{u}_{P+1},\ldots,\mathbf{u}_{2M+1}\} \quad (45)$$

Similarly, we get

$$span\{\mathbf{b}_1(\theta_1),\ldots,\mathbf{b}_1(\theta_P)\}=span\{\mathbf{v}_1,\ldots,\mathbf{v}_P\}$$
$$\perp span\{\mathbf{v}_{P+1},\ldots,\mathbf{v}_{2M}\} \quad (46)$$

From Eqs. (45) and (46), it is known that orthogonal signal subspace and noise subspace can be obtained from the singular vectors of $\mathbf{C}_1$. And the dimension of the signal subspace is P which is independent with the correlation of the sources. For $\mathbf{C}_2$, the same conclusion holds.

4.2. Maximum number of identified targets

For the transceiver MIMO radar, the maximum number of identified targets depends mainly on formulas (19) and (30). Since $\mathbf{B}$ is full column rank and $\overline{\mathbf{\Lambda}},\overline{\mathbf{\Lambda}}_1$ are full rank, the maximum rank of $\mathbf{C}$ in Eqs. (19) and (30) is $2M+1$. Obviously, the maximum number of targets depends on the maximum rank of $\mathbf{C}$. Considering the ESPRIT method we used, the maximum number of identified targets is $2M$. Similarly, for the independent transmitter and receiver MIMO radar, the maximum number of identified targets is $2MN+M+N$. From the analysis above, it is known that MIMO radar can identify more targets than its counterpart phased array, which can only identify $2N$ targets even if the sources are independent.

5. Simulation results

Consider a MIMO radar with 8 transmit antennas, one of which is just used in the presence of colored noise as shown in Fig. 1, and 7 receive antennas. Gold sequences, which have relatively ideal auto-correlation and cross-correlation property, are chosen as transmit baseband signals. The power of each transmit antenna E_t=1 and the period length of the Gold sequences is 256. The carrier frequency is 10 GHz. All coherent sources have identical Doppler frequency, so that the Doppler frequency has no effect on the proposed method. Assume that there are 200 coherent pulses in one CPI and 200 Monte-Carlo trials are carried out. The covariance matrix of the spatial colored noise is a complex symmetric Toeplitz matrix with $[1,0.9,\ldots 0.9^7]$ as the absolute value of its top row, and the power of the noise $\delta_n^2=1$. The signal-to-noise ratio (SNR) is defined as $10\log10(E_t\cdot|\beta|^2\cdot K/\delta_n^2)$ and the root mean square error (RMSE) of the ith target $\mathrm{RMSE}(\theta_i)=\sqrt{(1/M)\sum_{m=1}^{M}(\hat{\theta}_{im}-\theta_i)^2}$, where M is the Monte-Carlo trial number, $\hat{\theta}_{im}$ is the estimate of the mth experiment and θ_i is the true value. Experiments are implemented for the transceiver system and the independent transmitter and receiver system, respectively. For comparison, the corresponding results of the classical forward/backward smoothing method [3] (which we call FB method for brevity) are also given. For the transceiver system, the range-compressed data of each transmit waveform are treated as the data of the sub-array of the FB method; for the independent transmitter and receiver system, the data vector $\mathbf{y}_l$ in Eq. (31) is considered as the data of a linear array with 49 elements and the FB method in Ref. [3] is applied to it with the element number of the sub-array being 25. The MUSIC method in Ref. [3] is replaced by the SVD-based ESPRIT method for equity.

Experiment 1, the transceiver radar system with three coherent targets which have the same power and are located at $\theta_1=-5^\circ,\theta_2=10^\circ,\theta_3=35^\circ$ is considered, with both the spatial white and colored noise in consideration. Fig. 2 shows the plot of the target histogram of the proposed method with SNR=10 dB and Fig. 3 shows the plot of the RMSE versus SNR of the second target. It can be seen from Fig. 2 that the proposed method can successfully detect the targets in both white and colored noise circumstances. From Fig. 3, it is seen that, in white noise case, the proposed method attains better performance in low SNR and the same performance in high SNR compared with the FB method, which attributes to the complete de-correlation

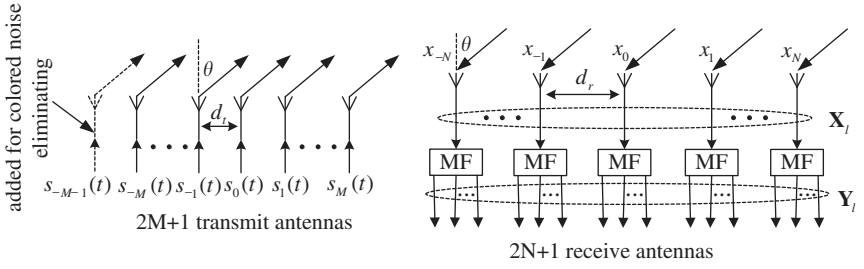

Fig. 1. Illustration of the considered mono-static MIMO radar system.

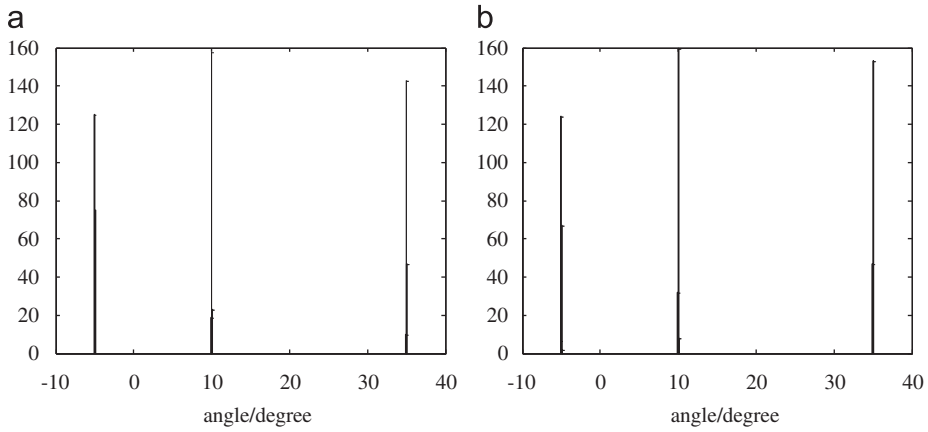

Fig. 2. Target histogram of the proposed method for transceiver radar system: SNR=10 dB: (a) white noise case and (b) colored noise case.

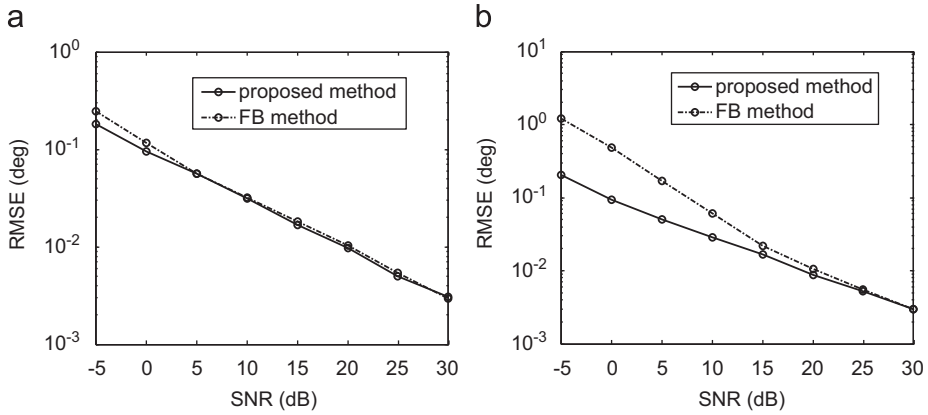

Fig. 3. RMSE and root CRB of the angle of the second target for transceiver radar system: (a) white noise case and (b) colored noise case.

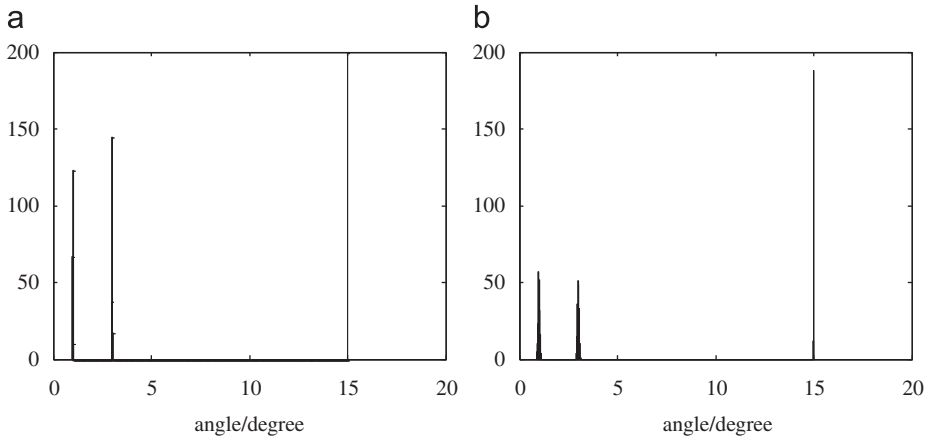

Fig. 4. Target histogram of the proposed method for independent transmitter and receiver radar: SNR=10 dB. (a) White noise case and (b) colored noise case.

capability of the proposed method. In the colored noise case, the performance of the proposed method is better, compared with the FB method, during wide SNR range, which shows the superiority of the proposed method in colored noise circumstance.

Experiment 2, the independent transmitter and receiver system with three coherent targets which have the same power and are located at $\theta_1 = 1^{\circ}, \theta_2 = 3^{\circ}, \theta_3 = 15^{\circ}$ is considered, with both the spatial white and colored noise in consideration. Fig. 4 shows the plot of the target

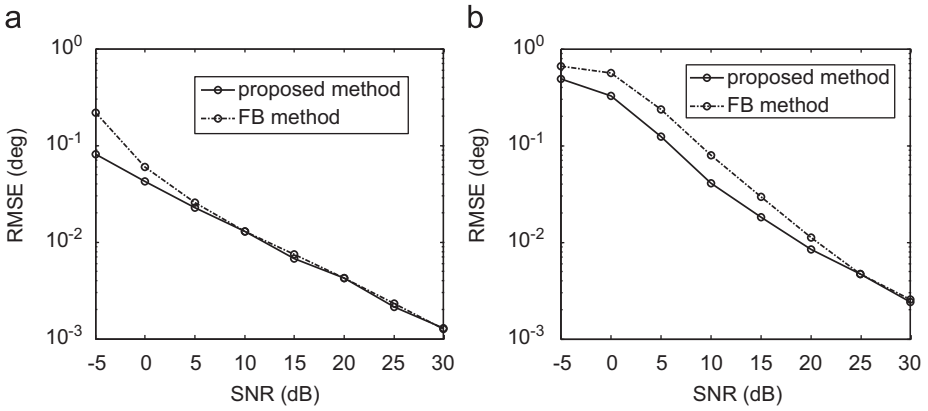

Fig. 5. RMSE and root CRB of the angle of the second target for independent transmitter and receiver radar: (a) white noise case and (b) colored noise case.

histogram of the proposed method with SNR=10 dB and Fig. 5 shows the plot of the RMSE versus SNR of the second target. From Fig. 4 it is also seen that, the proposed method can detect the targets in both the white and colored noise cases. Fig. 5 shows that, compared with the FB method, the proposed method owns better performance in low SNR for the white noise case and during wide SNR range for the colored noise case. Moreover, by comparing Fig. 5 with Fig. 3, it is observed that although the targets in Experiment 2 are much nearer than the targets in Experiment 1, the RMSE of the second target of Experiment 2 is nearly the same with that of Experiment 1, which shows that the independent transmitter and receiver system owns higher resolution compared with the transceiver radar system.

6. Conclusion

For the transceiver system, the independent transmitter and receiver system, the proposed method can successfully detect the targets. In the white noise environment, it performs better than the FB method in low SNR owing to its complete de-correlation capacity, and in the colored noise circumstance, it owns better performance over the FB method during wide SNR range since it can eliminate the colored noise while the FB method is helpless. Since the independent transmitter and receiver system has larger useful DOF over the transceiver system, it takes on higher resolution and can detect more targets. By capitalizing on the large DoF of MIMO radar, the transceiver system, the independent transmitter and receiver system can detect more targets than its counterpart phased array radar.

Acknowledgments

This paper is sponsored by National Nature Science Foundation of China (NSFC) under Grant 60736009, 60825104 and the Fundamental Research Funds for the Central Universities under Grant k50510020014. The work is also supported by the Program for Changjiang Scholars and Innovative Research Team in University (IRT0954). The authors are grateful to the anonymous reviewers for their valuable comments and suggestions which greatly improved the manuscript. Also the authors wish to thank the classmates who have given selflessness help in writing this paper.

References

[1] R.O. Schmidt, Multiple emitter location and signal parameter estimation, IEEE Transactions on Antennas and Propagation 34 (3) (1986) 276–280.
[2] R. Roy, T. Kailath, ESPRIT-a subspace rotation approach to estimate of parameters of cisoids in noise, IEEE Transactions on Acoustic Speech and Signal Processing 34 (10) (1986) 1340–1342.
[3] T.J. Shan, H.M. Wax, H.T. Kailath, On spatial smoothing for direction of arrival estimation of coherent signals, IEEE Transactions on Acoustic Speech and Signal Processing 33 (4) (1985) 806–811.
[4] W.X. Du, R.L. Kirlin, Improved spatial smoothing techniques for DOA estimation of coherent signals, IEEE Transactions on Signal Processing 39 (5) (May 1991) 1208–1210.
[5] B.H. Wang, Y.L. Wang, H. Chen, Weighted spatial smoothing for direction-of-arrival estimation of coherent signals, in: Proceedings of IEEE Antennas and Propagation Society International Symposium, San Antonio, Texas, 16–21, June, 2002, vol. 2, pp. 668–671.
[6] P. Stoica, B. Ottersten, M. Viberg, R.L. Moses, Maximum likelihood array processing for stochastic coherent sources, IEEE Transactions on Signal Processing 44 (1) (1996) 96–105.
[7] F.M. Han, X.D. Zhang, An ESPRIT-like algorithm for coherent DOA estimation, Antennas and Wireless Propagation Letters 4 (2005) 443–446.
[8] C. Zeng, G.S. Liao, Direction finding in the presence of coherent signals based on data matrix decomposition, Systems Engineering and Electronics 27 (4) (2005) 603–605 in Chinese.
[9] E. Fisher, A. Haimovich, R. Blum, L. Cimini, D. Chizhik, R. Valenzuela, Spatial diversity in radars- models and detection performance, IEEE Transactions on Signal Processing 54 (3) (2006) 823–838.
[10] A.M. Haimovich, R. Blum, L. Cimini, MIMO radar with widely separated antennas, IEEE Signal Processing Magazine 25 (1) (2008) 116–129.
[11] I. Bekkerman, J. Tabrikian, Target detection and localization using MIMO radars and sonars, IEEE Transactions on Signal Processing 54 (10) (2006) 3873–3883.
[12] J. Li, P. Stoica, W. Roberts, On parameter identifiability of MIMO radar, IEEE Signal Process Letters 14 (12) (2007) 968–971.
[13] L.Z. Xu, J. Li, P. Stoica, Target detection and parameter estimation for MIMO radar systems, IEEE Transactions on AES 44 (3) (2008) 927–939 July.
[14] J. Li, P. Stoica, MIMO radar with colocated antennas, IEEE Signal Processing Magazine (2007) 106–114 Sep.

[15] L. Xu, J. Li, P. Stoica, Radar imaging via adaptive MIMO techniques, in: Proceedings of the European Signal Processing Conference, Florence, Italy, Sep. 2006.
[16] M. Jin, G.S. Liao, J. Li, Joint DOD and DOA estimation for bistatic MIMO radar, Signal Processing 89 (2009) 244–251.
[17] J.L. Chen, H. Gu, W.M. Su, A new method for joint DOD and DOA estimation in bistatic MIMO radar, Signal Processing 90 (2010) 714–718.
[18] C. Duofang, C. Baixiao, Q. Guodong, Angle estimation using ESPRIT in MIMO radar, Electronics Letters 44 (12) (2008) 5th June.
[19] P.Z. Fan, N. Suehiro, N. Kuroyanagi, X.M. Deng, Class of binary sequences with zero correlation zone, Electron Letters 35 (10) (1999) 777–779.
[20] X.D. Zhang, Y.C. Liang, Prefiltering-based ESPRIT for estimating parameters of sinusoids in non-Gaussian ARMA noise, IEEE Transactions on Signal Processing 43 (1995) 349–353.